

Original Research Article**Initial insight to effect of exercise on maximum pressure in the aortic root using 2D fluid-structure interaction model****Abstract**

Study of maximum pressure in the left ventricle (MPLV) has already been a challenging aspect of clinical diagnosis. The aim of this study was to propose a model to estimate the maximum pressure in the left ventricle (MPLV) for a healthy subject based on cardiac outputs measured by echo-Doppler (non-invasive) and catheterization (invasive) techniques at rest and during exercise.

Blood flow through aortic valve was measured by Doppler flow echocardiography. Aortic valve geometry was calculated by echocardiographic imaging. A Fluid-Structure Interaction (FSI) simulation was performed, using an Arbitrary Lagrangian-Eulerian (ALE) mesh. Boundary conditions were defined as pressure loads on ventricular and aortic sides during ejection phase. The FSI simulation can be used to determine a numerical relationship between the cardiac output to aortic diastolic and left ventricular pressures. This relationship enables the prediction of pressure loads from cardiac outputs measured by invasive and non-invasive clinical methods. Ventricular systolic pressure peak that was calculated from cardiac output of Doppler method, Fick oximetric and Thermodilution method lead to a 82.1%, 95.6% and 147% increment throughout exercise, respectively. The mean slopes obtained from curves of ventricular systolic pressure based on Doppler, Fick oximetric and Thermodilution methods are 1.27, 1.85 and 2.65 mmHg/heart rate, respectively. Our predicted Fick-MPLV values were lower 8% to 19%, Thermodilution-MPLV ones 17% to 25% ,and Doppler-MPLV ones 57% to 73% when compared to clinical reports. Since flow depends on the pressure loads, measuring more accurate intraventricular pressures helps to understand the

25 cardiac flow dynamics for better clinical diagnosis. Furthermore, the method is noninvasive,
26 safe, cheap and more practical. As clinical Fick-measured values have been known to be
27 more accurate, our Fick-based prediction could be the most applicable.

28 **Key words:** maximum pressure in the left ventricle, Fluid-Solid interaction, Fick oximetric,
29 Thermodilution.

30 **1. Introduction**

31 Cardiac disease is a major cause of death in industrialized countries, in spite of advances in
32 prevention, diagnosis, and therapy [1]. Despite challenging aspects of clinical diagnosis, the
33 investigation of maximum pressure in the left ventricle (MPLV) assessment is among the
34 most clinically important [2]. Therefore, detecting MPLV during blood pumping is important
35 for recognition of such diseases. This study has used a Fluid-Structure Interaction (FSI)
36 model to predict MPLV and trans-aortic pressure. Common invasive techniques like Fick
37 oximetric and Thermodilution have associated risks [4]. MPLV measurements were first
38 examined using invasive catheters [5]. Brenner et al. studied the MPLV at peak which was
39 estimated in five infants using echo-Doppler and catheterisation method [6]. Greenberg et al.
40 progressed a method to evaluate the MPLV by analyzing intraventricular flow velocities [7].
41 Firstenberg et al [8] and Tonti et al [9] non-invasively determined correlations between the
42 earlier invasive MPLV measurements. Few studies have estimated MPLV with respect to
43 the heart rate variations during exercise. However, heart rate changes during exercise,
44 simultaneous intraventricular pressure gradients and ejection flow patterns have been
45 measured by a multisensor catheter at rest and exercise [10]. Redaelli and Montevocchi
46 studied only intraventricular pressure gradients using fluid structure interaction at a heart
47 heart rate of 72 bpm. Without using an exercise protocol [11] Clavin et al and Spinelli et al
48 used an electrical model to assess cardiac function based on left intraventricular-impedance
49 at rest condition [12, 13].

50 Experimentally, intraventricular pressure is a valuable measurement. Nonetheless, due to the
51 fact that the heart is not perfused via the normal route, intraventricular pressure cannot be
52 measured even with sophisticated medical instruments like an open-ended catheter [14].
53 These studies demonstrated the importance of pressure measurement to make certain efficient
54 LV performances.

55 FSI simulations are overall well matched to cardiovascular modeling [15 , 16]. This method
56 requires the use of an Arbitrary Lagrange-Euler (ALE) mesh to analyze both structural
57 deformation and fluid flow; i.e. Computational Fluid Dynamics and Finite Element Analysis
58 [17 , 18]. Recently, FSI has been used to investigate heart valves [19 ,20 , 21 , 22 , 23 , 24
59 ,25 , 26]. Previously we have measured the cardiac output and stroke volume for a healthy
60 subject by coupling an echo-Doppler method with a fluid-structure interaction simulation at
61 rest and during exercise and particular attention was given to validating the model versus
62 measures of cardiac function that could be reliably calculated by applying clinical protocols,
63 with varying exercise [27] and the effect of exercise on blood flow hemodynamic including
64 the change of flow patterns across the aortic valve, vorticity, shear rate, stress and strain on
65 the leaflets while exercise [28]. In our previous studies pressures across the aorta were
66 measured and applied to models. However, accurate predictions of aortic pressures are only
67 possible using invasive techniques. Numerical calculation method is a useful tool for
68 prediction of the real pressure values and it can analyze how different parameters, like
69 material properties, affect output . It also has a potential role in clinical diagnosis.

70 The aim of this study is to predict MPLV by numerical derivation from the relationship of
71 cardiac output to MPLV [27] from invasive clinical cardiac output measurement [29]. First,
72 the relationship between Cardiac output and systolic ventricular pressure and systolic aortic
73 pressure is derived, based on our previous numerical study [27]. Additionally, Christie et
74 al.[29] clinically obtained equations for Thermodilution cardiac output (COT) and Fick

75 oximetric cardiac output (COF) to Doppler cardiac output (COD). Therefore, COT and COF
 76 were measured for the subject [27]. Then, MPLV was calculated noting to the numerical
 77 relationship among cardiac output, systolic ventricular pressure and systolic aortic pressure.

78

79 **2. Methods**

80

81 **2.1 Overview**

82 We have presented our two-dimensional FSI aortic valve model previously [27 , 28]. The
 83 model, as well as clinical measurements, are briefly described in section 2.2. Section 2.3
 84 presents the methods to calculate to derive pressure predictions based on cardiac output.

85

86 **2.2 Combined clinical and numerical approach**

87 A healthy male, aged 33, with normal cardiovascular function had his hemodynamic data
 88 recorded while rest and exercise. Informed consent was acquired for the participant in line
 89 with accepted procedures approved by the Department of Cardiovascular Imaging (Shaheed
 90 Rajaei Cardiovascular, Medical and Research Center, Tehran, Iran). Hemodynamic data was
 91 assessed from maximal bicycle exercise tests and Doppler ECG. Systolic and diastolic
 92 pressures of the brachial artery were measured and related to heart rate changes at rest and
 93 exercise (Figure 1). Equations 1 and 2 were used to determine the central aortic pressure from
 94 brachial aortic pressure measurements. This relationship was previously determined by
 95 comparing brachial pressure (acquired by Oscillometry) to the central pressure acquired using
 96 an invasive method [30].

$$97 \quad \text{Central systolic pressure} = \text{Brachial systolic pressure} + 2.25 \quad 1$$

$$98 \quad \text{Central diastolic pressure} = \text{Brachial diastolic pressure} - 5.45 \quad 2$$

99 where all pressures were measured in *mmHg*.

100 Left ventricular systolic pressure was derived from the calculated central systolic pressure.
101 Previously, a pressure difference of around 5 mmHg was found between peak left ventricular
102 systolic pressure and central systolic pressure, using catheterization [31]. The ejection times
103 were derived from Doppler-flow imaging under B-mode.

104 The aortic valve geometry simulated is presented in figure 2 and dimensions are
105 provided in table 1. Briefly, dimensions were obtained with respect to T-wave of ECG
106 (maximum opening area), with diameters of the aortic valve annulus and the sinus valsalva
107 measured at the peak T-wave time using a resting para-sternal long-axis view. The two cusps
108 were considered to be isotropic, homogenous and to have a linear stress-strain relationship.
109 This assumption has been used in other heart valve models [20, 23, 24, 32]. Blood was
110 assumed to be an incompressible and Newtonian fluid [16]. All material properties are
111 provided in table 2 and were obtained from the literature [33, 34].
112 For fluid boundaries (figure 2), pressure was applied at the inflow boundary of the aortic root
113 at the left ventricular side. A moving ALE mesh was used which enabled the deformation of
114 the fluid mesh to be tracked without the need for re-meshing [35]. Second order Lagrangian
115 elements were used to define the mesh. The mesh contained a total of 7001 elements (Figures
116 3a and 3b). The finite element analysis package Comsol Multi-physics (v4.2) was used to
117 solve the FSI model under time dependent conditions [23, 24, 36]. The fluid velocity is
118 coupled to the structural deformation while the valve is loaded by the fluid, this ensures
119 simultaneous coupling [37, 38, 39].

120

121 **2.3 Cardiac output**

122 Regression equations were used to calculate Left ventricular systolic pressure (VSP; equation
123 3) and Aortic diastolic pressure (ADP; equation 4) from the cardiac output predicted
124 numerically (figure 4). :

$$125 \quad VSP = 1.266E - 06 * (CO)^2 - 0.017 * (CO) + 152.3 ; (R^2=0.997) \quad (3)$$

$$126 \quad ADP = 5.915E - 07 * (CO)^2 - 0.014 * (CO) + 142.2 ; (R^2=0.965) \quad (4)$$

127 Previously we extracted the relationship between Doppler cardiac output and heart rate using
128 equation 5 [27 , 40]:

$$129 \quad COD = -0.498 * (Hr)^2 + 213.550 * (Hr) - 6164 ; (R^2 = 0.995) \quad (5)$$

130 Christie et al. (1987) obtained regression equations for the relationship between
131 Thermodilution cardiac output (COT) and Fick oximetric cardiac output (COF) to Doppler
132 cardiac output (COD), based on the data given from 15 subjects:

$$133 \quad COT = 1.41 * COD - 2394 \quad (6)$$

$$134 \quad COF = 1.03 * COD + 2165 \quad (7)$$

135 Combining equations (6) and (7) with equation (5) by applying Matlab (2010), we have
136 extracted the following relations and shown the curves of Fick oximetric (COF) and
137 Thermodilution cardiac output (COF) relative to the heart rate in Figure 5.

$$138 \quad COT = -0.705 * (Hr)^2 + 301.796 * (Hr) - 11131; (R^2 = 0.995) \quad (8)$$

$$139 \quad COF = -0.515 * (Hr)^2 + 220.461 * (Hr) - 4217; (R^2 = 0.995) \quad (9)$$

140

141 Combining equations (3) and (4) with equation (8), enables left ventricular systolic and aortic
142 diastolic pressures to be plotted with respect to heart rate respectively, based on

143 Thermodilution method. These plots are shown for our subject in figures 6 and 7. Also,

144 Combining equations (3) and (4) with equation (9) enables us to plot left ventricular systolic

145 and aortic diastolic pressures with heart rate, respectively. The plots derived from a Fick

146 oximetric method for our subject are shown in figures 6 and 7. Combining equations (3) and

147 (4) with equation (5), enables the plotting of left ventricular systolic and aortic diastolic

148 pressures with respect to heart rate, respectively. The plots derived from the use of a Doppler

149 method for our subject are shown in figures 6 and 7.

150 **3. Results**

151 Aortic diastolic pressure, derived from Doppler based measurements, increased by 13.4%,
152 corresponding to 8.7 mmHg, with increasing heart rate from 98 bpm to 169 bpm. Instead,
153 using the Fick oximetric method a 42%, corresponding to 26.7 mmHg, increase was
154 calculated. Whereas Thermodilution led to a prediction of a 62.6% increase, corresponding to
155 39.6 mmHg. The mean slopes obtained from curves of aortic diastolic pressure based on
156 Doppler, Fick oximetric and Thermodilution methods were 0.14, 0.40 and 0.60 (mmHg/heart
157 rate), respectively.

158 The ventricular systolic pressure, predicted from the Doppler method, increased 82.1%,
159 corresponding to 87.2 mmHg, with increasing heart rate from 98 bpm to 169 bpm (figure 7).
160 This increase was calculated to be 95.6%, corresponding to 127.9 mmHg, using the Fick
161 oximetric method and 147% (or 181.6 mmHg) for the Thermodilution method. The mean
162 slopes obtained from curves of ventricular systolic pressure based on Doppler, Fick oximetric
163 and Thermodilution methods are 1.27, 1.85 and 2.65 (mmHg/heart rate) respectively.

164

165 **4. Discussion**

166

167 **4.1 Study findings**

168 The study has combined FSI hemodynamic measurements of the cardiac output, from a
169 healthy subject [27] with invasive clinical measurements [29] in order to estimation of
170 maximum pressure in the left ventricles during exercise. Despite using a simplified two-
171 dimensional model, the method developed has potential for clinical application (section 4.2)
172 and the obtained values show good agreement with the literature (see section 4.3). Moreover,
173 the FSI model reliably predicted MPLV over a range of heart rates based on clinical
174 measurement of cardiac outputs. MPLV was calculated by cardiac output of Doppler method,

175 Fick oximetric and Thermodilution method which shows 82.1%, 95.6% and 147%
176 increment during exercise. Since cardiac output calculated with Fick method eliminates the
177 plights associated with measuring VO₂ precisely and do not require either an assumption of
178 or measurement of the respiratory exchange ratio, that may prove to be more clinically useful
179 for continuous cardiac output monitoring than Thermodilution cardiac [41, 42]. In this regard
180 we can say that our Fick-based results could be more precise than the other two methods.
181 Christie et al, furthermore, reported the advantage of Doppler measurement is its operational
182 feasibility, although its outputs can be modified by the correlation equations between that and
183 invasive techniques [29].
184 The mean slopes which were derived from curves of ventricular systolic pressure are 1.27,
185 1.85 and 2.65 (mmHg/heart rate). This validation involved comparison numerical and clinical
186 results for cardiac output and stroke volume. Such methods are well-founded when
187 combining a model with experimental measurement [29 , 30 , 43 , 44].

188

189 **4.2 Clinical application & reliability**

190 Predicting reliable intraventricular pressures is important in clinical diagnosis and treatment
191 [2]. For instance, One of the recent commercially available medical investigating devices to
192 assess intraventricular pressure has a fluid-filled, balloon-tipped catheter that is intended for
193 insertion into the ventricle [14]. The balloon provides a closed system from which
194 intraventricular pressure is determined. The balloon is attached to a fluid-filled catheter and
195 connected to a pressure transducer and bridge amplifier [14]. This highly advanced method
196 clearly demonstrates its involved risk and because of that they are mostly applicable for
197 animal studies due to their invasive method.

198 The presented non invasive method let us predict more accurate MPLV by measuring
199 brachial pressures of subjects. Our numerical estimations based on Fick oximetric have

200 potential for clinical application (8% to 19% underestimation when compared to clinical
201 approaches; see discussion, Comparison to literature), this is important because Fick
202 methods' evaluations have been reported to be more accurate than other clinical approaches
203 [41, 42]. Catheterization-Thermodilution , the current gold-standard for measuring
204 intraventricular pressure [4], is an invasive procedure with potential risks such as heart
205 failure, cardiac arrhythmia, and even death [4]. Moreover, Thermodilution exposes the
206 patient and doctor to radiation. Exercising while catheterized results in a range of practical
207 problems too, therefore, is not common customary action. However, the use of a numerical
208 method permits the estimation of cardiac function by non-invasive measurements during an
209 exercise protocol. Therefore, the key-concern is the dependability of numerical methods
210 when predicting MPLV while exercise. Yet, computational methods have not been combined
211 with non-invasive clinical measurements to predict a patient's MPLV. Our model enables
212 assessment of cardiac function and hemodynamic changes from rest to exercise [27 , 28]. It
213 was feasible to derive the relationship for cardiac output to MPLV. Concerning invasive
214 clinical cardiac output measurement as more accurate [29], we are able to estimate more
215 precise MPLV. It should be mentioned that most of clinical measurement of MPLV have
216 done for animals like dog such as Monroe study [45] due to the risk associated with them.
217 It is generally accepted that cardiovascular modelling is mechanical-based system, in
218 particular when the mechanical characteristic (e.g. MPLV) is intended to investigate. In this
219 point of view, development of such mechanical simulations can be resulted in more accurate
220 prediction of cardiovascular performance. By this it is thought that electrical-based
221 simulations are more limited and less useful as compared to mechanical-based modelling.
222 Based on our current knowledge, Max pressure of left ventricle, for example, has not been
223 studied yet by electrical-based modelling.
224

225 **4.3 Comparison to literature**

226 Following a literature search we have not found a previous comparable study that combined a
227 clinical and numerical approach to predict MPLV during exercise. In our study, the patient
228 specific MPLV were predicted at a range of heart rates induced by exercise for echo-Doppler,
229 Thermodilution , and Fick oximetric methods. While the variation for MPLV from rest to
230 peak of external work is established [3] this is the first study to use numerical methods to
231 predict these values for an individual. Textbook MPLV range from 80 (mmHg) at 70 bpm to
232 270 mmHg at 180 bpm. It can also be approximateed that the slope of MPLV is about 2.2
233 mmHg/heart rate for non athletes during exercise [3]. Our subject is also a nonathlete. Our
234 Thermodilution-based prediction is overestimated by 17%, our Fick oximetric-based
235 prediction is underestimated by 19% and our Doppler prediction is underestimated by 73%
236 when compared to textbook values.

237 Loeppky et al. clinically investigated the systolic blood pressure changes while exercise for
238 ten subjects. The mean slope of MPLV over the exercise protocol roughly was 2
239 mmHg/Heart rate [46]. Our Thermodilution-based estimation is overestimated by 25%, our
240 Fick oximetric-based estimations is underestimated by 8% and our Doppler-based estimation
241 is underestimated by 57% when compared to the results from Loeppky et al.

242 Compared to published values [3, 46], our results based on Thermodilution method are
243 overestimated by 17% to 25%, the Fick oximetric method underestimates values by 8% to
244 19% and the Doppler method leads to underestimates of 57% to 73% when compared to
245 clinical data.

246 Fick methods' evaluations has been reported to be more accurate [41, 42]. Hence, our
247 numerical estimations based on Fick oximetric are more reliable when it is considered that an
248 8% to 19% underestimation could be due to our considered limitations for the numerical
249 model or that only single subject was investigated. Textbook maximum systolic pressure for

250 the normal left ventricle range from 250 to 300 mmHg, but varies widely among different
251 subjects with heart strength and degree of heart stimulation by cardiac nerves. [10] MPLV
252 has been studied by catheterization. MPLV ranged between 121 (mmHg) at the heart rate of
253 75 bpm to 210 (mmHg) at 180 bpm. They reported the average of MPLV of 6 patients with
254 normal left ventricular function and no valve abnormalities, was 121 (mmHg) at 75 bpm at
255 rest to 149 (mmHg) at 108 bpm during exercise. Although our study is numerical and based
256 on one subject, our model predicted MPLV would be useful to quantify how closely the
257 values match the literature.

258

259 **4.4 Limitations & future trends**

260 A fully developed discussion of the limitations of the FSI model has been explained
261 previously [27]. In short, the main limitations are that:

- 262 ▪ simplifications of the mechanical properties, plus using a constant orifice area and a
263 single diameter for the ascending aorta in the model;
- 264 ▪ statistical and generalized data was applied for clinical determination of
265 hemodynamic;
- 266 ▪ Instead of three-dimensional structure a two-dimensional model was used to
267 investigate;

268 Despite model limitations we previously presented excellent agreement with clinical
269 measurements and the general literature [27]. A real model as three-dimensional could
270 results more precise predictions, while, it would also increase the solution time (currently less
271 than 15 minutes). This would hold disadvantages for clinical applications, yet, it is required
272 to be balanced against the short solution time for a 2D FSI model. Our model solution time is
273 potentially able to be translated into clinical practise, moreover, ameliorating of solution time

274 can be possible with more robust computer power. Furthermore, a range of values for
275 statistical comparison are not predictable without the including variability in models [24]. At
276 this time, there is a tendency towards patient specific models, like [47], due to potential
277 profits in aiding treatment/diagnosis for an individual. Prediction of intraventricular pressure
278 could be useful to construct more reliable heart valve prototypes [48].
279 Although pattern pressure of left ventricle is imposed by its walls contraction, we predicted
280 this with comparing the underestimated numerical values of cardiac output [27] with that of
281 invasive clinical reports [29]. Needless to say, this underestimation resulted from pressures
282 of boundary conditions. Consequently, they were studied to be modified to correspond with
283 clinical approaches.

284

285 **5. Conclusions**

286 We introduced a two-dimensional model of aortic valve which is able to predict maximum
287 pressure in the left ventricles during exercise using fluid-structure interaction. The model was
288 analyzed against results from echo-Doppler, Thermodilution and Fick oximetric methods as
289 invasive and non-invasive clinical methods. The model has potential applications in the
290 prediction of ventricular pressures. As clinical Fick-measured values have been suggested as
291 most accurate, our Fick-based predictions are likely the most applicable.

292

293 **6. Competing interests**

294 The authors of the manuscript declare that they have no conflict of interest.

295

296

297

298 **References**

- 299 1. Murphy SL, Xu J: Deaths: Preliminary Data for 2010, National Vital Statistics Reports
300 2012 4(60):31, 2010.
- 301 2. Bonow RO, Mann DL, Zipes DP, Libby P, Book Braunwald's Heart Disease: A
302 Textbook of Cardiovascular Medicine 9th ed, Philadelphia, Pa: Saunders Elsevier
303 2011.
- 304 3. Guyton. AC, Hall JE, Textbook of Medical Physiology, Philadelphia PA, WB Saunders
305 P:27, 1996.
- 306 4. Lavdaniti M, , *Int J Caring Sci* 1(3):112–117, 2008.
- 307 5. Courtois MA, Kovacs SJ, Ludbrook PA, Physiologic early diastolic intraventricular
308 pressure gradient is lost during acute myocardial ischemia, *Circulation* 82:1413–23,
309 1990.
- 310 6. Brenner JI, Baker KR, Berman MA: Prediction of left ventricular pressure in infants
311 with aortic stenosis. *Br Heart J* 44(4):406-10, 1980.
- 312 7. Greenberg NL, Vandervoort PM, Thomas JD, Instantaneous diastolic transmitral
313 pressure differences from color Doppler M mode echocardiography, *Am J Physiol*
314 271:H1267–76, 1996.
- 315 8. Firstenberg MS, Vandervoort PM, Greenberg NL, et al, Noninvasive estimation of
316 transmitral pressure drop across the normal mitral valve in humans: importance of
317 convective and inertial forces during left ventricular filling, *J Am Coll Cardiol*
318 36:1942–9, 2000.
- 319 9. Tonti G, Pedrizzetti G, Trambaiolo P, Salustri A, Space and time dependency of
320 inertial and convective contribution to the transmitral pressure drop during ventricular
321 filling, *J Am Coll Cardiol* 38:290–1, 2001.
- 322 10. Pasipoularides A, Murgu JP, Miller JW, Craig WE, Nonobstructive left ventricular
323 ejection pressure gradients in man, *Circ Res* 61(2):220-7, 1987.

- 324 11 Redaelli A, and Montevicchi FM, Computational evaluation of intraventricular
325 pressure gradients based on a fluid-structure approach, *Journal of Biomechanical*
326 *Engineering*, transactions of the ASME 118 (4): 529–537, 1996.
- 327 12. Clavin OE, Spinelli JC, Alonso H, Solarz P, Valentinuzzi ME, Pichel RH, Left
328 intraventricular pressure–impedance diagrams (DPZ) to assess cardiac function. Part
329 1: morphology and potential sources of artifacts, *Med Progn Technol* 11: 17–24,
330 1986.
- 331 13. Spinelli JC, Clavin OE, Cabrera EI, Chatruc MR, Pichel RH, Valentinuzzi ME, Left
332 intraventricular pressure–impedance diagrams (DPZ) to assess cardiac function. Part
333 II: determination of end-systolic loci. *Med Progn Technol* 11: 25–32, 1986.
- 334 14. Intraventricular Pressure Measurement in a Langendorff Preparation,
335 <http://www.adinstruments.com/files/techniques/TN-BalloonCatheter.pdf>
- 336 15 . Bellhouse BJ, The fluid mechanics of heart valves. In: *Book Cardiovascular fluid*
337 *mechanics*, Volume 1, Bergel DH (ed), London Academic Press, 1972.
- 338 16 . Caro CG, Pedley TJ, Schroter RC, Seed WA, *Book The mechanics of the circulation*,
339 Oxford: Oxford University Press, 1978.
- 340 17 . Donea J, Giuliani S, Halleux JP, An arbitrary Lagrangian–Eulerian finite element
341 method for transient dynamic fluid–structure interactions, *Comput Methods Appl*
342 *Mech Engrg* 33(1-3):689 –723, 1982.
- 343 18 . Formaggia L, Nobile F, A stability analysis for the arbitrary Lagrangian Eulerian
344 formulation with finite elements, *East–West J Numer Math*7(2):105–132, 1999.
- 345 19 . Al-Atabi M, Espino DM, Hukins DWL, Computer and experimental modelling of
346 blood flow through the mitral valve of the heart, *J Biomech Sci Eng* 5(1):78-84, 2010.
- 347 20 . De Hart J, Peters GW, Schruers PJ, Baaijens FP, A two-dimensional fluid-structure
348 interaction model of the aortic valve, *J Biomech* 33(9):1079-1088, 2000.

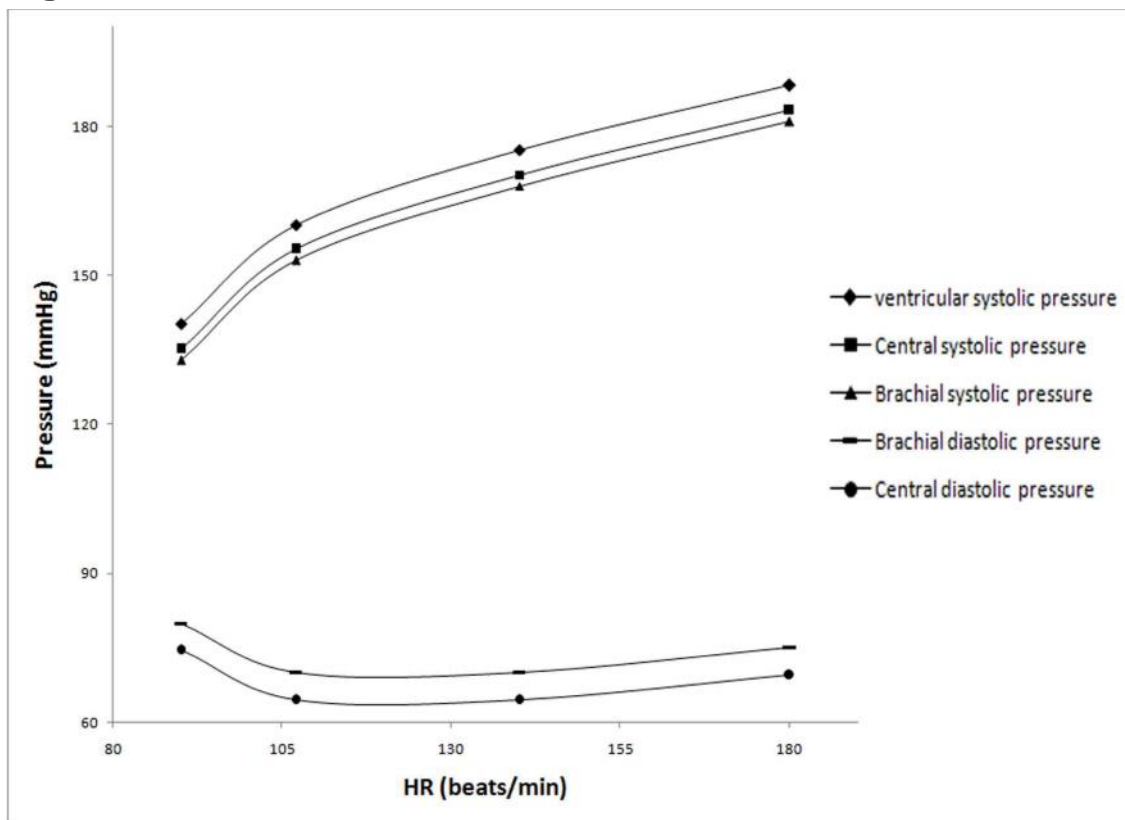
- 349 21 . De Hart J, Peters GW, Schreurs PJ, Baaijens FP, A three-dimensional computational
350 analysis of fluid–structure interaction in the aortic valve, *J Biomech* 36(1):103-112,
351 2003a.
- 352 22 . De Hart J, Baaijens FP, Peters GW, Schreurs PJ, A computational fluid-structure
353 interaction analysis of a fiber-reinforced stentless aortic valve, *J Biomech* 36(5):699-
354 712, 2003b.
- 355 23 . Espino DM, Shepherd DET, Hukins DWL, Evaluation of a transient, simultaneous,
356 Arbitrary Lagrange Euler based multi-physics method for simulating the mitral heart
357 valve, *Comput Methods Biomech Biomed Engin* In Press. DOI:
358 10.1080/10255842.2012.688818, 2012a.
- 359 24 . Espino DM, Shepherd DET, Hukins DWL, A simple method for contact modelling
360 in an arbitrary frame of reference within multiphysics software, *J Mech*, In Press
361 DOI: 10.1017/jmech.2012.128 , 2012b.
- 362 25 . Stijnen JMA, De Hart J, Bovendeerd PHM, Van de Vosse FN, Evaluation of a
363 fictitious domain method for predicting dynamic response of mechanical heart valves,
364 *J Fluids Struct* 19(6):835-850, 2004.
- 365 26 . Xia .G.H, Zhao .Y and Yeo .J.H , Numerical Simulation of 3D Fluid-Structure
366 Interaction Using AN Immersed Membrane Method, *Modern Physics Letters B*
367 19(28-29):1447-1450. 2005
- 368 27 . Bahraseman HG, Hassani K, Navidbakhsh M, Espino DM, Sani ZA, Fatourae N,
369 Effect of exercise on blood flow through the aortic valve: a combined clinical and
370 numerical study. *Comput Methods Biomech Biomed Engin*, In Press. DOI:
371 10.1080/10255842.2013.771179, 2013.

- 372 28 . Bahraseman HG, Hassani K, Navidbakhsh M, Espino DM, Fatourae N, Combining
373 numerical and clinical methods to assess aortic valve hemodynamics during exercise,
374 *Journal of Engineering in Medicine, Part H* In revision, 2012b.
- 375 29 . Christie J, Sheldahl LM, Tristani FE, Sagar KB, Ptacin MJ, Wann S, Determination
376 of stroke volume and cardiac output during exercise: comparison of two-dimensional
377 and Doppler echocardiography, Fick oximetry, and Thermodilution , *Circulation*
378 76(3):539-547, 1987.
- 379 30 . Park SH, Lee SJ, Kim JY, Kim MJ, Lee JY, Cho AR, Lee HG, Lee SW, Shin WY,
380 Jin DK, Direct Comparison between Brachial Pressure Obtained by Oscillometric
381 Method and Central Pressure Using Invasive Method, *Soonchunhyang Medical*
382 *Science* 17(2):65-71, 2011.
- 383 31 . Laske A, Jenni R, Maloigne M, Vassalli G, Bertel O, Turina MI, Pressure gradients
384 across bileaflet aortic valves by direct measurement and echocardiography, *Ann*
385 *Thorac Surg* 61(1):48-57, 1996.
- 386 32 . Weinberg EJ, Kaazempur-Mofrad MR, A multiscale computational comparison of
387 the bicuspid and tricuspid aortic valves in relation to calcific aortic stenosis, *J*
388 *Biomech* 41(16):3482–3487, 2008.
- 389 33 . Govindarajan V, Udaykumar H.S, Herbertson L.H, Deutsch S, Manning K.B, and
390 Chandran K.B, Two-Dimensional FSI Simulation of Closing Dynamics of a Tilting
391 Disk Mechanical Heart Valve, *J. Med. Devices* 4(1): 011001(1-11), 2010.
- 392 34 . Koch TM, Reddy BD, Zilla P, Franz T, Aortic valve leaflet mechanical properties
393 facilitate diastolic valve function, *Comput Methods Biomech Biomed Engin*
394 13(2):225-34, 2010.
- 395 35 . Winslow AM, Numerical solution of the quasilinear poisson equation in a
396 nonuniform triangle mesh, *J Comput Phys* 1(2):149-172, 1966.

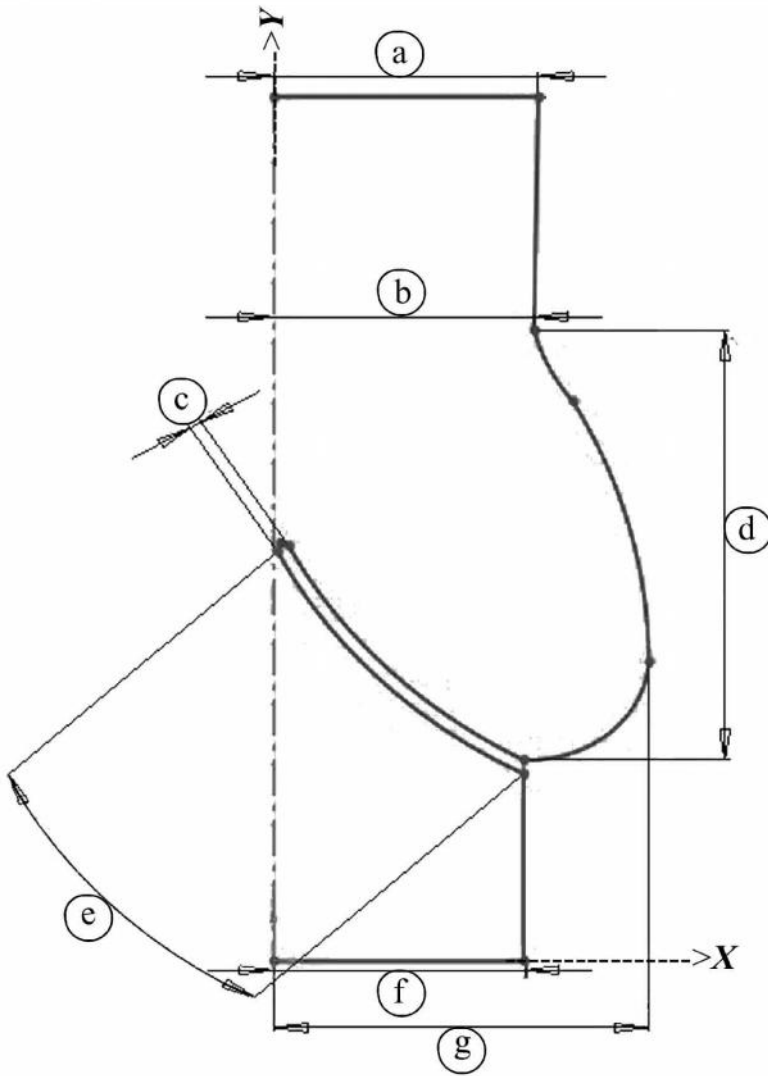
- 397 36 . Espino DM, Shepherd DET, Hukins DWL, Development of a transient large strain
398 contact method for biological heart valve simulations, *Comput Methods Biomech*
399 *Biomed Engin* 16(4):413-424, 2013.
- 400 37 . Dowell EH, Hall KC, Modelling of fluid-structure interaction, *Annu Rev Fluid Mech*
401 33(1):445-490, 2001.
- 402 38 . Wall W, Gerstenberger A, Gamnitzer P, Forster C, Ramm E, Large deformation
403 fluid-structure interaction – advances in ALE methods and new fixed grid approaches
404 *In: Fluid-structure interaction*, Bungartz HJ, Shafer M (Eds.) Berlin: Springer, 2006.
- 405 39 . Van de Vosse FN, De Hart J, Van Oijen CHGA, Bessems D, Gunther TWM, Segal
406 A, Wolters BJB, Stijnen JMA, Baaijens FPT, Finite-element-based computational
407 methods for cardiovascular fluid-structure interaction, *J Eng Math* 47(3-4):335–368,
408 2003.
- 409 40 . MATLAB version 7.10.0, Natick, Massachusetts, The MathWorks Inc, 2010.
- 410 41. Mahutte CK, Jaffe MB, Chen PA, Sasse SA, Wong DH, Sasso CS, Oxygen Fick
411 and modified carbon dioxide Fick cardiac outputs, *Crit Care Med* 22(1):86-95, 1994.
- 412 42. Jarvis SS, Levine BD, Prisk GK, Shykoff BE, Elliott AR, Rosow E, Blomqvist CG,
413 Pawelczyk JA, Simultaneous determination of the accuracy and precision of closed-
414 circuit cardiac output rebreathing techniques, *J Appl Physiol* 103(3):867-74. Epub
415 2007 Jun 7, 2007.
- 416 43 . Maroni JM, Oelberg DA, Pappagianopoulos P, Boucher CA, Systrom DM,
417 Maximum Cardiac Output During Incremental Exercise by First-pass Radionuclide
418 Ventriculography, *Chest* 114(2):457-461, 1998.
- 419 44 .Sugawara J, Tanabe T, Miyachi M, Yamamoto K, Takahashi K, Iemitsu M, Otsuki T,
420 Homma S, Maeda S, Ajisaka R, Matsuda M, Non-invasive assessment of cardiac
421 output during exercise in healthy young humans: comparison between Modelflow

- 422 method and Doppler echocardiography method, *Acta Physiol Scand* 179(4):361–366,
423 2003.
- 424 45 . Monroe RG, La Farge CG, Gamble WJ, Hammond RP, Gamboa R, Left ventricular
425 performance and blood catecholamine levels in the isolated heart, *Am J Physiol*
426 211(5):124854, 1966.
- 427 46. Loeppky JA, Gurney B, Kobayashi Y, Icenogle MV. Effects of ischemic training on
428 leg exercise endurance, *J Rehabil Res Dev* 42(4):511-22, 2005.
- 429 47 . Öhman C, Espino DM, Heinmann T, Baleani M, Delingette H, Viceconti M, Subject-
430 specific knee joint model: Design of an experiment to validate a multi-body finite
431 element model, *Visual Comp* 27(2):153-159, 2011.
- 432 48. Janko F Verhey, corresponding author, Nadia S Nathan, Otto Rienhoff, Ron Kikinis,
433 Fabian Rakebrandt, and Michael N D'Ambra, Finite-element-method (FEM) model
434 generation of time-resolved 3D echocardiographic geometry data for mitral-valve
435 volumetry, *Biomed Eng Online* 5: 17. Published online 2006 March 3. doi:
436 10.1186/1475-925X-5-17, 2006.

437 **Figures**



438 Figure 1 - Interpolated curves for brachial, central and ventricular pressures.
 439

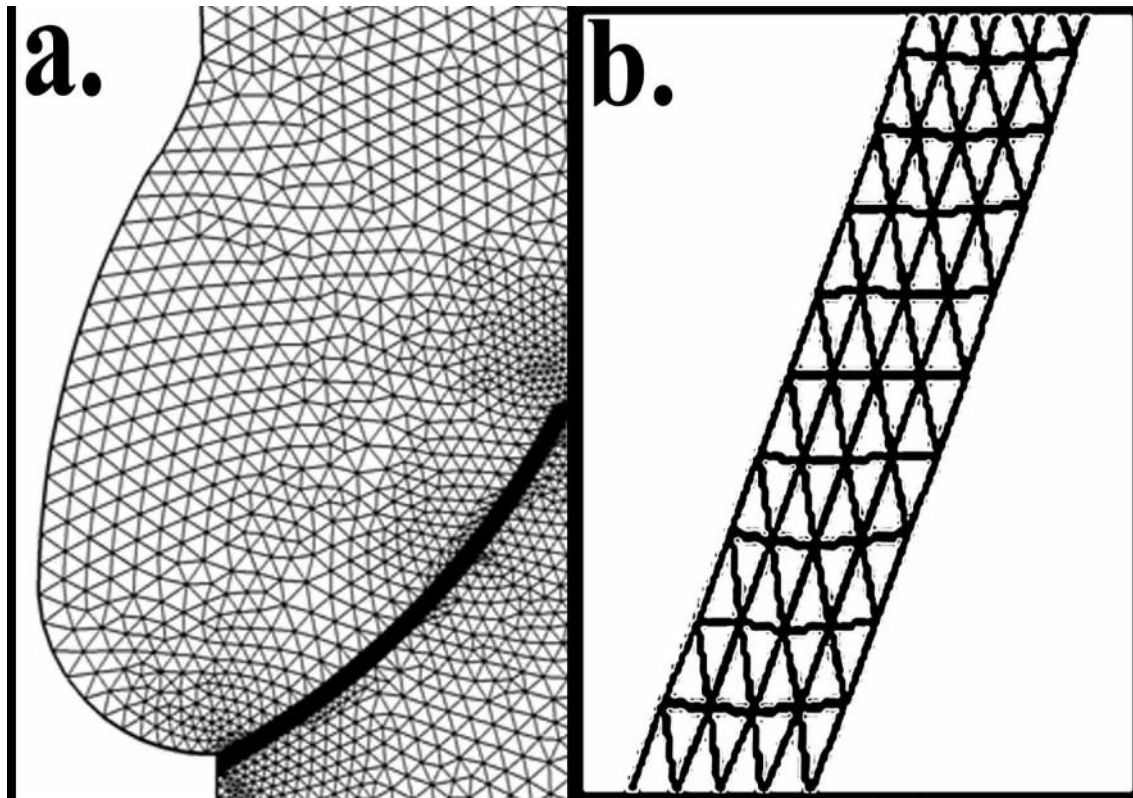


440

441 **Figure 2** - a) Ascending aorta radial after sinotubular site; b) Aortic side radial; c) Leaflet

442 thickness; d) Valve height; e) Leaflet length; f) Ventricular side radial; g) Maximum radial of

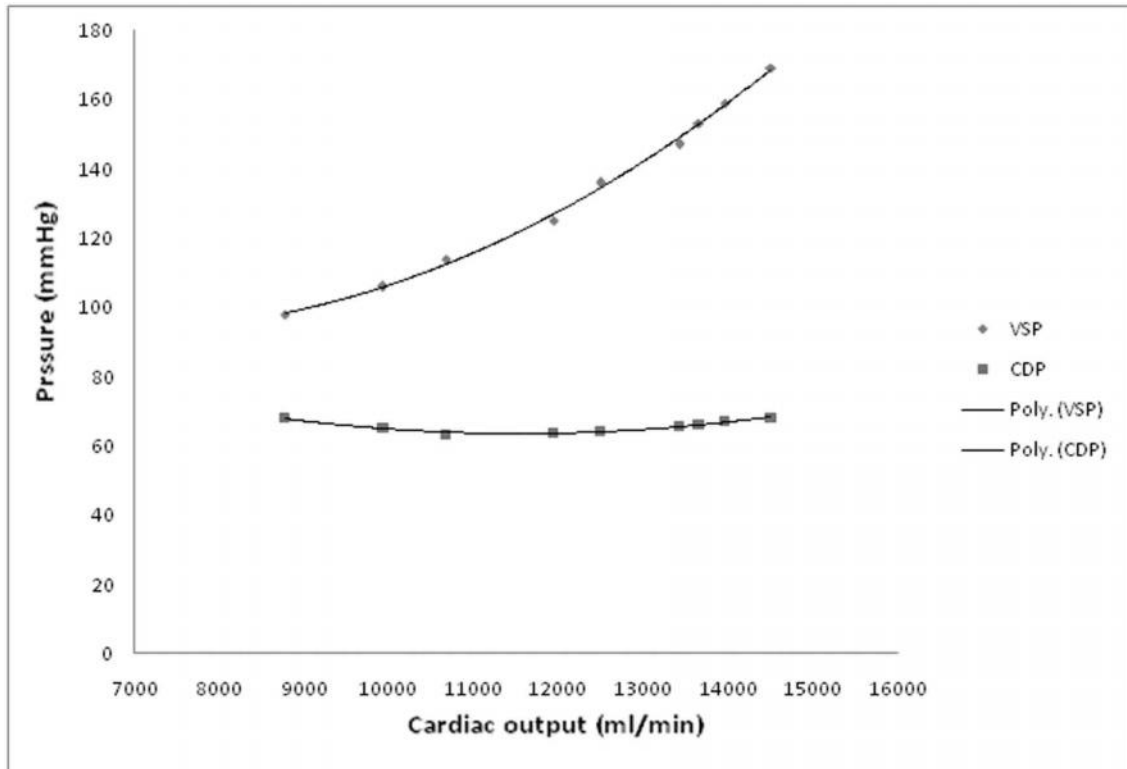
443 normal aortic root.



444

445 **Figure 3 - Mesh for the (a) the fluid domain mesh generation valve cusps and (b)**
446 **elements on a cusp of the solid domain mesh generation.**
447

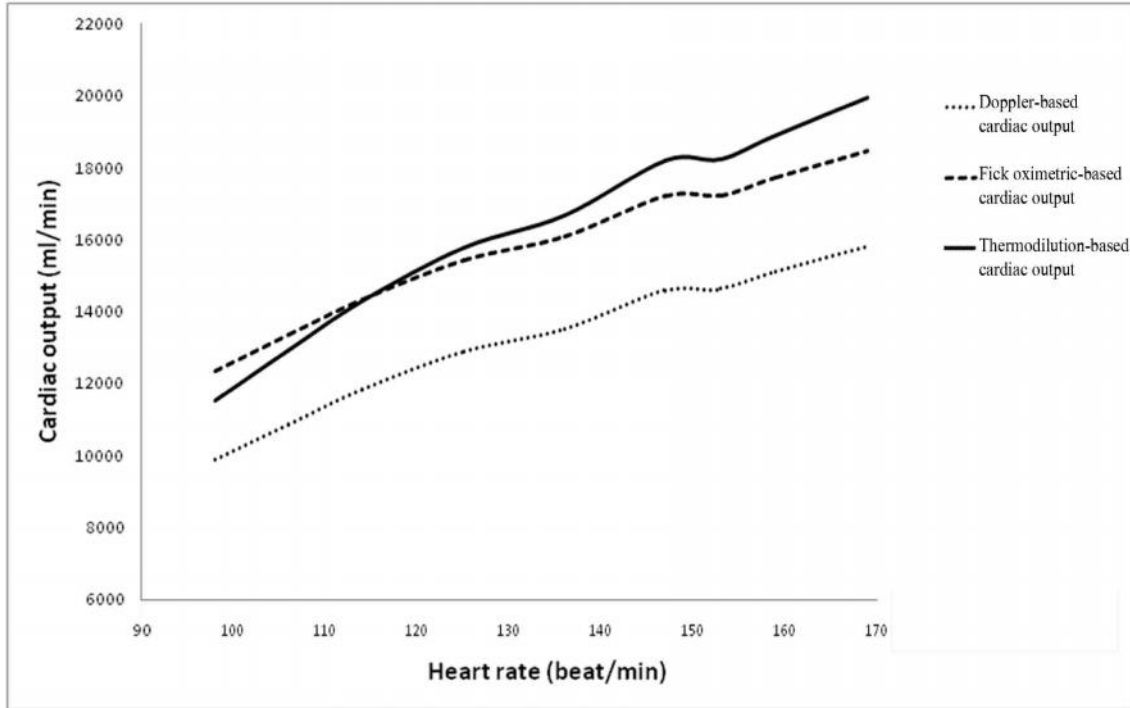
448
449



450
451
452
453
454

Figure 4 - Ventricular systolic pressure (VSP) and Aortic diastolic pressure (ADP) to cardiac output that were plotted for numerical method.

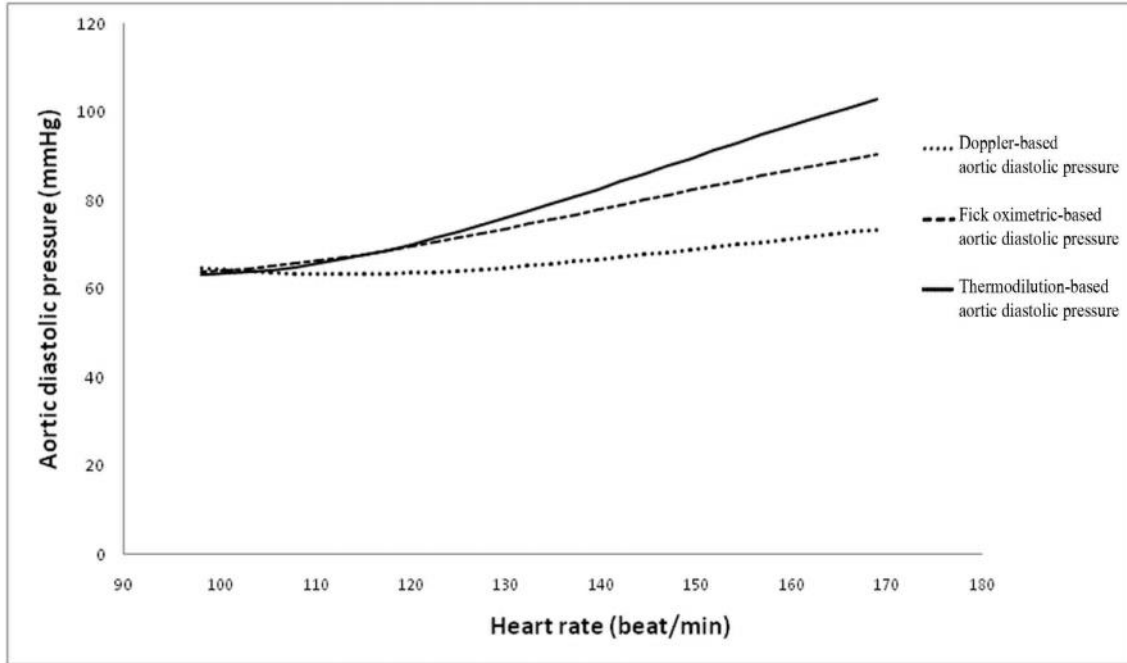
455



456
457
458
459
460
461

Figure 5 – FSI prediction of cardiac output’s change relative to heart rate based on Doppler method (round dot line), Fick oximetric method (square dot line), Thermodilution method (solid line).

462



463

464

465

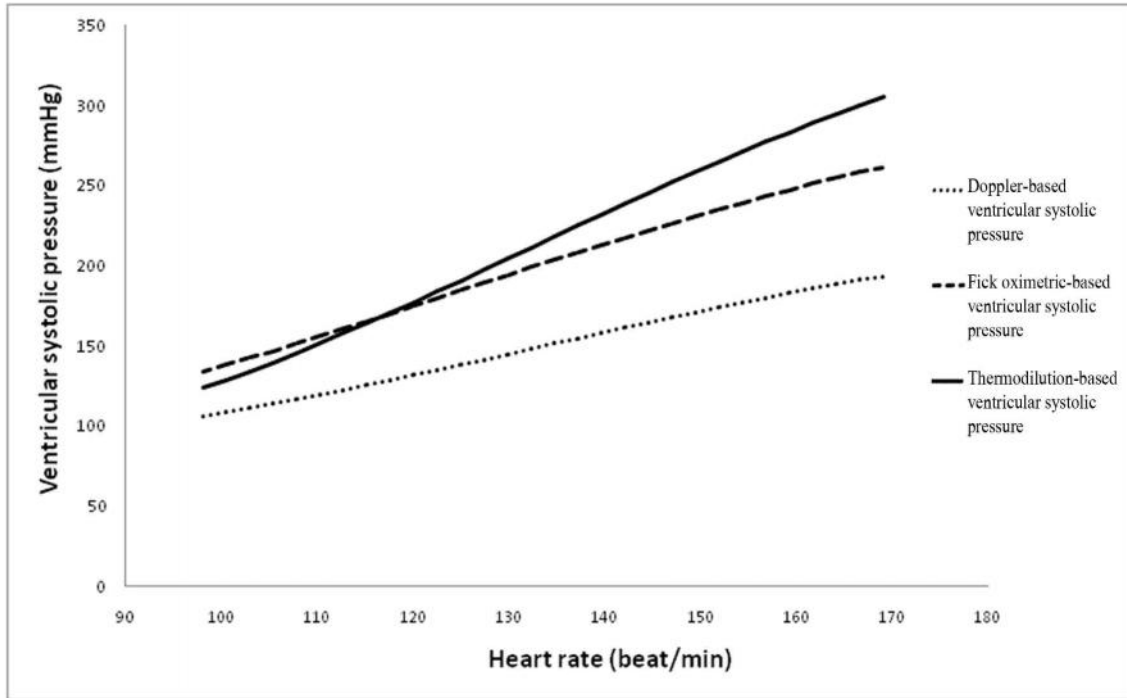
466

467

468

Figure 6- FSI prediction of aortic diastolic pressure's change relative to heart rate based on Doppler method (round dot line), Fick oximetric method (square dot line), Thermodilution method (solid line).

469



470

471

472

473

474

Figure 7 - FSI prediction of ventricular systolic pressure's change relative to heart rate based on Doppler method (round dot line), Fick oximetric method (square dot line), Thermodilution method (solid line).

475 **Tables**476 **Table 1 - Geometric parameters of the aortic valve as shown in figure 2.**

(a)	(b)	(c)	(d)	(e)	(f)	(g)
Ascending aorta radius after sinotubular junction (mm)	Aortic side radius (mm)	Leaflet's thickness (mm)	Valve's height (mm)	Leaflet's length (mm)	Ventricular side radius (mm)	Maximum radius of normal aortic root (mm)
11.75	11.5	0.6	20.36	16.6	11.1	16.65

477

478

479 **Table 2 - Mechanical properties.**

Viscosity (Pa.s)	Density (kg/m ³)	Young's modulus (N/m ²)	Poisson ratio
3.5×10^{-3}	1056	6.885×10^6	0.4999

480

481

482